Water Science & Technology

IWA PUBLISHING

Water Science & Technology Vol 87 No 9, 2233 doi: 10.2166/wst.2023.134

Study of synthesis and characterization of raw bagasse, its char and activated carbon prepared using chemical additive

Ekta R. Raut [a,b,*], Monita A. Bedmohata (Thakur) [c] and Archana R. Chaudhari [d]

[a] G H Raisoni University, Amravati, 444701, India
[b] G H Raisoni College of Engineering, Nagpur, 440016, India
[c] Department of Applied Sciences, G H Raisoni University, Amravati, 444701, India
[d] Priyadarshini Bhagwati College of Engineering, Nagpur 440024, India
*Corresponding author. E-mail: ekta.raut@raisoni.net

ERR, 0000-0002-6172-1149; MAB, 0000-0001-8050-4812; ARC, 0000-0001-6694-6497

ABSTRACT

This paper reports the use of naturally available raw material as sugarcane bagasse (SB) to prepare cost-effective activated carbon. Activated carbon preparation from SB by using $ZnCl_2$ was carried out by chemical activation method. The raw bagasse, its char and activated carbon were characterized on the basis of iodine number, carbon, hydrogen, nitrogen analysis, Fourier-transform infrared spectroscopy (FTIR), scanning electron microscopy (SEM), thermogravimetric analysis (TGA) and Brunauer–Emmett–Teller (BET) surface area to check their effectiveness. During activated carbon synthesis, the impregnation ratio of SB and $ZnCl_2$ was maintained at 1:1–1:3 and activation temperature was in the range of 600–900 °C for 1 h. From the characterization study, the highest iodine adsorption of activated carbon was found to be 1140.69 mg/g with a 1:2 ratio at 900 °C whereas char gives an iodine number of 529.63 mg/g at the same temperature. The BET surface area of raw bagasse, its char and activated carbon (SB-Zn_2-900) obtained was 4.30, 514.27 and 1386.58 m^2/g, respectively, which shows charrification and chemical activation improves surface area. The optimum ratio of impregnation and activation temperature was found to be 1:2 at 900 °C. In this work, activated carbon was successfully prepared and obtained product has better characteristics than previously reported studies.

Key words: activating agent, activation, agricultural waste, char, impregnation

HIGHLIGHTS

- Utilization of agricultural waste material for production of value-added material such as activated carbon.
- Minimizes the burden of solid waste management.
- Prepared activated carbon can be utilized for pollutant removal.
- Minimizes water pollution by adsorption.
- Can replace expensive commercial activated carbon.

1. INTRODUCTION

The role of the agricultural sector in human and economic development cannot be overemphasized. The impact of agricultural solid waste on human and animal well-being as well as on the environment is substantial, which is mainly due to ignorance during managing agricultural solid waste. A lot of lignocellulosic biomass is created every year causing environmental issues and hence, one can convert agro-waste into net worth products. This step can promote the utilization of sustainable raw materials in a proper way (Hon & Siraishi 2000; Obi *et al.* 2016).

Due to an incessant demand for commercial activated carbon (AC) for industrial applications, the market cost of commercial activated carbon reached $1,100–1,500/tons. Hence, the preparation of activated carbon from cheap and easily available raw materials can make it cost-effective (Hock & Zaini 2018). One such agricultural waste is sugarcane bagasse (SB) which is used to synthesize biomass waste-based activated carbon in this study.

SB is the residue left after the extraction of sugarcane juice and it contains 35% of cellulose, 25% of hemicellulose and 22% of lignin (Rezende *et al.* 2011). SB is treated as a potential material for energy recovery. Once it has been processed properly, it can be used as a carbon-neutral energy material (Ramajo-Escalera *et al.* 2006; Hofsetz & Silva 2012; Dantas *et al.* 2013). SB is used as a fuel in sugar plants for the generation of steam and in ethanol distillation (Nunes *et al.* 2020). It is used in the production of derived fuels using gasification and rapid pyrolysis (Naik *et al.* 2010). It is also used in the paper and pulp industry for the manufacturing of corrugated boards (Samariha & Khakifirooz 2011). Due to its wide range of uses, it is no longer considered a waste nowadays. Due to high lignocellulosic content, its usefulness in the form of char and activated carbon is capturing researchers' attention. The microporous structure of any activated carbon is due to its high cellulose and low lignin content (Misran *et al.* 2018; Dwiyaniti *et al.* 2020).

The term 'char' represents the solid residue that forms after thermal degradation of carbon-rich agricultural waste in limited oxygen conditions. It consists of organic material with a composition varying from barely carbonized agricultural waste at low temperatures to a highly carbonized material at high temperatures. The physical and chemical characteristics of biochar depend on the temperature used for pyrolysis and the type of biomass used. It can be used to improve contaminated soil quality, soil productivity, removal of toxic metals and production of bio-fuel, etc. (Kumar & Bhattacharya 2018). Activation of biochar can also be found useful in removing particular contaminants from water.

There are various methods used for the removal of pollutants removal from liquid or gaseous phases like membrane filtration, precipitation and coagulation, reverse osmosis distillation, adsorption, ion-exchange, photochemical degradation, biological degradation and chemical oxidation (Rashed 2013; Raut *et al.* 2021). Amongst these methods, the adsorption of organic as well as inorganic impurities with activated carbon is gaining importance and has been widely used (Harry & Francisco 2006). It has been found to be an economical and effective treatment method because of no sludge formation (Ioannidou & Zabaniotou 2007).

Activated carbons are porous materials with rich porosity and larger surface area with greater adsorption capacity (Paraskeva *et al.* 2008; Oubagaranadin & Murthy 2012). Activated carbons possess a large internal surface area in the range of 500–2,000 m^2/g (Chisutia *et al.* 2014). Activated carbon synthesis can be carried out by two methods: physical and chemical activation. Physical activation (Salgado *et al.* 2018) involves the carbonization of a precursor followed by activation. CO_2 or steam gasifying agents were used as a medium of activation. Carbonization is carried out between 400 and 850 °C and activation is carried out between 600 and 900 °C. This method will help to form new functional groups which enhance the sorption properties of the char. These gasifying agents will extract carbon from the network of porous carbon given in the following reactions:

$$CO_2 + C \rightarrow 2CO \quad (1)$$

$$H_2O + C \rightarrow CO + H_2 \quad (2)$$

In chemical activation, the precursor was impregnated with a chemical agent followed by activation. The activating agents that can be used are H_3PO_4, $ZnCl_2$, KOH, NaOH, Na_2CO_3, K_2CO_3 and H_2SO_4 (Hayashi *et al.* 2002; Demiral *et al.* 2008; Kalderis *et al.* 2008; Gardare *et al.* 2015; Ghani *et al.* 2017). The AC is washed with hydrochloric acid followed by deionized water and dried for further use.

This study discusses the synthesis and characterization of char and $ZnCl_2$ made activated carbon. The effect of activation temperature and impregnation ratio on yield and iodine number was studied and discussed. The raw bagasse (precursor), char and activated carbon were characterized by iodine number, CHN analysis, Fourier-transform infrared spectroscopy (FTIR), scanning electron microscopy (SEM), thermogravimetric analysis (TGA-DTA) and Brunauer–Emmett–Teller (BET) surface area and elemental analysis energy-dispersive spectroscopy (EDS).

This study focuses on activated carbon preparation and its comparison with raw bagasse and bagasse char. Such types of comparative studies based on raw stage, char stage and activated carbon stage have not been extensively studied earlier, hence this study discusses the thermochemical conversion of bagasse into char and activated carbon.

2. EXPERIMENTAL

2.1. Materials

Raw SB was collected from Manas Agro Industries (Umrer, India). Analytical (AR) grade chemicals used were dry $ZnCl_2$ (EMPLURA), $Na_2S_2O_3$ (EMPLURA), Merk Life Science, Pvt Ltd (Worli, Mumbai), resublime iodine (Q24904), KI (Loba Chemie Pvt. Ltd, Jehangir Villa, Colaba, Mumbai), HCl & starch (Fisher Scientific, Thermo Electron LLS India Pvt, Sion

(East), Mumbai), purchased from Vaishnavi Scientific & Trading Company (Ayodhya Nagar, Nagpur, India). Instruments used were heating mantle (Bio Technics India, Mumbai), electric muffle furnace (Tempo Instruments, Mumbai), pH meter (Deluxe pH-101), digital balance (Citizon) and laboratory oven (BTI).

2.2. Methods

2.2.1. Production of SB char

Raw SB was washed and dried in an oven for 1 h at 110 °C. The dried bagasse was then cut into small pieces. The dried bagasse was kept in a muffle furnace at four different temperatures ranging from 600 to 900 °C. In the absence of an inert atmosphere, no ash was formed in obtained char. The prepared char was washed with deionized water, dried in an oven at 110 °C for 1 h and packed in an air-tight container for further use. The resulting chars were labeled as SBC600, SBC700, SBC800 and SBC900 which denote SB char at 600, 700, 800 and 900 °C. Figures 1 and 2 show raw SB and its char, respectively.

Figure 1 | Sugarcane bagasse.

Figure 2 | Sugarcane bagasse char.

2.2.2. Production of sugarcane bagasse activated carbon

The sugarcane bagasse (SB) obtained from the source was washed with water for the removal of impurities and dried in sunlight for 5 days. SB was cut into small pieces and allowed to dry in a laboratory hot air oven for 1 h at 110 °C. The impregnation of bagasse with $ZnCl_2$ was carried out on a heating mantle. For a 1:1 ratio, a known amount of SB was taken in a glass beaker. An equal amount of solid $ZnCl_2$ in a known volume of distilled water was dissolved in another beaker. $ZnCl_2$ solution in bagasse was added and the contents were mixed. This mixture was kept on a heating mantle at 80 °C until it turned into a paste (Ekpete *et al.* 2017). After 24 h, the impregnated material was kept in a muffle furnace (Tempo Instruments, Mumbai) for 1 h at 600 °C. During activation, between temperatures of 300–600 °C, gaseous products start releasing from the outlet pipe with maximum fumes. Above 600 °C, the removal of fumes stopped. The major observation after activation and cooling of the furnace was no ash formation in the prepared product. The prepared carbons were washed with 1 M HCl followed by hot deionized water until neutral pH was reached. The washed material of activated carbon was dried in an oven at 110 °C for 1 h and ground with the help of an iron rod. The ground powder was sieved through an ASTM-70 test sieve and packed in an air-tight container for further use. The activation procedure for ratios 1:2 (wt/wt) and 1:3 (wt/wt) was the same at four different temperatures from 600 to 900 °C. The resulting carbons so prepared were labeled as SB-Zn_1-600, SB-Zn_1-700, SB-Zn_1-800, SB-Zn_1-900, SB-Zn_2-600, SB-Zn_2-700, SB-Zn_2-800, SB-Zn_2-900, SB-Zn_3-600, SB-Zn_3-700, SB-Zn_3-800, SB-Zn_3-900, which denotes SB $ZnCl_2$ followed by ratio 1:1, 1:2, 1:3 and activation temperature. The yield of activated carbon is calculated by the following equation:

$$\% \text{ yield} = \frac{W_1}{W_2} \times 100 \tag{3}$$

where W_1 is the weight of activated carbon, W_2 is the weight of raw material taken.

3. CHARACTERIZATION

The raw SB, its char and activated carbon were characterized by iodine number which is an indication of the micro-porosity of activated carbon. It is determined as per ASTM: D4607-94 standard method. CHN analysis was carried out by using a ThermoFinnigan analyzer available at the Department of CIL, Punjab University, Chandigarh. The thermal decomposition of material was tested by TGA by using DTG-60 simultaneous DTA-TG apparatus. The functional group availability of the surface of activated carbon was recorded by FTIR by using an IR-Affinity-1 spectrometer. The amorphous or crystalline nature of activated carbon was studied by powder X-ray diffraction studies (XRD) by using 'Rigaku' Miniflex diffractrometer. The surface structure of activated carbon was studied by scanning electron microscope (JEOL-6380A).

4. RESULTS AND DISCUSSION

4.1. Yield of activated carbon and char

From Table 1, it is observed that activation reduces the mass of produced carbon and char. The percentage of mass loss increases with the increase in ratio and temperature. As soon as the activation temperature increases, the yield of activated carbon decreases, as shown in Table 1. The decrease in yield indicates the evolution of more volatile matter at higher temperatures (Foo & Hameed 2011). The same observation was reported by Lua & Ting (2004). Loss in weight also represents the reaction mechanism carried out between lignocellulosic material and chemical agent (Angin *et al.* 2013). In $ZnCl_2$ activation, the aqueous solution is entered into the carbon skeleton to produce pores at a temperature above its melting point. The reaction between the carbon atoms and $ZnCl_2$ is promoted in the inner layers of the carbon. The use of $ZnCl_2$ as a chemical agent generally increases the carbon content through the formation of aromatic graphitic structures (Hock & Zaini 2018). During activation, it has been observed that around 400 °C of the removal of most volatile matter gets started like CO and CO_2 due to the effect of activation. During the initial stage of thermal degradation from 400 to 600 °C, zinc chloride is completely dehydrated from water molecules taken by bagasse (Bouchemal *et al.* 2015). Also, it takes off H_2 and O_2 atoms from the carbon structure to form H_2O molecules (Cartula *et al.* 1990). The activated carbon with the highest yield of 31.87% was obtained at 600 °C for the ratio 1:1. It has been observed from the experimental work that as the impregnation ratio increases, yield decreases. This is because at higher ratios, swelling and elasticity increase. This indicates that there may be an additional oxidation reaction occurring during impregnation with the removal of volatile matter (Hamza *et al.* 2015). The yield of

Table 1 | Percentage yield and loss of SB activated carbon (SBAC) SBAC

Sample code	% Yield	% Loss
SB-Zn_1-600	31.87	68.13
SB-Zn_1-700	28.73	71.27
SB-Zn_1-800	26.53	73.47
SB-Zn_1-900	20.27	79.73
SB-Zn_2-600	28.53	71.47
SB-Zn_2-700	25.60	74.4
SB-Zn_2-800	22.34	77.66
SB-Zn_2-900	18.23	81.77
SB-Zn_3-600	25.12	74.88
SB-Zn_3-700	20.66	79.34
SB-Zn_3-800	18.22	81.78
SB-Zn_3-900	16.31	83.69
SBC600	45.06	54.94
SBC700	37.83	62.17
SBC800	22.72	77.28
SBC900	12.94	87.06

prepared chars also decreases with increasing activation temperature. The percentage yield and loss of activated carbon and char at different temperatures are presented in Table 1.

4.2. Characterization

4.2.1. Iodine number determination

Iodine numbers of activated carbon measure the approximate surface area and micro-pore volume. The iodine number of activated carbon and char was determined in the laboratory as per ASTM D 4607-94 standard method (Standard Test Method 2006). The milligram of I_2 adsorbed on the surface of 1 g activated carbon when the iodine concentration of residual filtrate is 0.02 N. All the required solutions of I_2, 10% HCl, sodium thiosulfate, potassium iodide and starch indicator were prepared in the laboratory with distilled water.

In this method, 1 g of activated carbon sample was taken in a 250 mL conical flask. Ten mL of 5% of HCl solution was added to it. The flask was then kept on a hot plate for boiling for 30 s. The flask was allowed to cool and 100 mL of 0.1 N iodine solution was added to it. The conical flask was immediately covered and shaking of contents for 30 s was carried out. The contents were filtered using filter paper immediately after the shaking period. The initial 20–30 mL of filtrate was discarded and a further 50 mL of filtrate was titrated with 0.1 N sodium thiosulfate by using starch as an indicator until the solution changes to colorless.

It can be seen from Table 2 that, in the case of SB char, the iodine number increases as the impregnation ratio increases from 1:1 to 1:3. The bagasse char gives iodine numbers of 496.17, 500.81, 504.12 and 510.75 mg/g at 600, 700, 800 and 900 °C, respectively. The maximum iodine number (510.75 mg/g) was found at 900 °C. In the case of activated carbon, the iodine number decreases first from 1:1 to 1:2 ratio from 600 to 800 °C. However, at 900 °C, as the impregnation ratio increases from 1:1 to 1:2, the iodine number increases and from 1:2 to 1:3, it decreases. The highest iodine number (1,140.69 mg/g) was obtained at 900 °C for a 1:2 ratio. Hence, the optimum impregnation ratio (bagasse: zinc chloride) was found to be 1:2. Char without activation provides a lesser iodine number than activated carbon (SB-Zn_2-900). This proves that activation by using chemical reagents enhances iodine numbers and adsorption capacity.

All the prepared samples at four different temperatures with three impregnation ratios were tested for iodine number. However, the char and activated carbon with the highest iodine number are only characterized further for FTIR, XRD, SEM and BET. Hence, based on the iodine number determined, SBC900 and SB-Zn_2-900 (1:2 ratio at 900 °C) were found to have the highest iodine number and therefore further characterization was carried out for FTIR, XRD, SEM and BET.

Table 2 | Iodine number of SBAC and SBC

Sample code	Iodine number (mg/g)
SB-Zn_1-600	970.09
SB-Zn_2-600	839.80
SB-Zn_3-600	1,062.94
SB-Zn_1-700	771.27
SB-Zn_2-700	995.37
SB-Zn_3-700	1,079.37
SB-Zn_1-800	952.91
SB-Zn_2-800	1,019.44
SB-Zn_3-800	952.91
SB-Zn_1-900	928.12
SB-Zn_2-900	1,140.69
SB-Zn_3-900	920.30
SBC600	496.17
SBC700	500.81
SBC800	504.12
SBC900	510.75

4.2.2. CHN analysis of raw bagasse, bagasse char and activated carbon

Elemental analysis works on the basic principle of oxidation of C, H, N and S into gases like CO_2, H_2O and SO_2 that are then separated by the chromatographic method. In this method, an accurately weighed sample was introduced in the furnace in the presence of a constant supply of inert gases (He). Oxygen gas is injected into the inert gas stream with a sample and allowed to combust in a tin capsule. The exothermic reaction takes place with the evolution of combustion gases which raised the furnace temperature from 1,000 to 1,800 °C within a short time. The combustion gases then swept through a series of oxidation columns containing agents like chromium oxide, tungsten trioxide, cobaltic oxide, etc., which ensures complete combustion of C, H, N and S into CO_2, H_2O and SO_2. The unreacted oxygen was then consumed by metallic copper present in the reduction column which was maintained at 700 °C and nitrogen-containing components were reduced to N_2. Separation of individual gases is carried out in the chromatographic column containing porous polymer maintained at less than 100 °C. Each element was then quantified by the signal generated during its sequential passage through a thermal conductivity detector (TCD) yielding a peak in abundance at different times (Michael *et al.* 2017). Elemental analysis was carried out on a ThermoFinnigan analyzer available at the Department of CIL, Punjab University, Chandigarh. The CHN analysis of raw bagasse, its char and activated carbon (SB-Zn_2-900) is shown in Table 3.

4.2.3. Thermogravimetric and differential thermal analysis of raw bagasse, bagasse char & activated carbon

The thermal decomposition of raw material was tested by TGA-DTA analysis. TGA was carried out on DTG-60 simultaneous DTA-TG apparatus (SHIMADZU CORP. 00812), available at RTMNU, Nagpur. In this analysis, samples were heated in an inert environment like nitrogen (flow rate 20 mL/min) at a controlled rate of 10 °C/min up to 900 °C. The temperature was

Table 3 | CHN analysis of raw SB, SBAC and SBC

Samples	% Carbon	% Hydrogen	% Nitrogen
Raw SB	42.049	5.538	0.106
Sugarcane bagasse char (SBC)	48.150	2.076	0.018
SB-Zn_2-900	80.126	3.569	1.873

raised at a constant rate for a known weight of sample and changes in weights were recorded as a function of temperature at different time intervals. The plot of change in weight with respect to temperature is plotted as a thermogram.

The decomposition of raw bagasse was observed in three stages. In the first stage, the removal of moisture takes place below 150 °C (Hanum *et al.* 2017), in the second stage, the decomposition of cellulose and lignin were observed in the range of 250–400 °C and in the third stage the curves become flat above 400 °C. This was due to the aromatization of lignin and at this stage, less weight loss occurs. Raw SB decomposition is shown in Figure 3.

The decomposition of char with increasing temperature is shown in Figure 4. In the case of char, in the range of 100–400 °C, an almost flat curve was observed and above 400 °C considerable weight loss occurs up to 600 °C. Above 600 °C, very little weight loss was observed, as shown in Figure 4.

Activated carbon shows moisture removal up to 150 °C. The major decomposition process occurs between 200 and 400 °C with a weight loss of approximately 70%wt (Wereko-Brobby & Hagen 1996). Above 600 °C, little weight loss was found as per the TGA curve shown in Figure 5. At lower temperatures, decomposition of lignocellulosic material takes place and at higher temperatures, lignin decomposes, as shown in Figure 5.

4.2.4. Fourier-transform infrared spectroscopy of raw bagasse, char and activated carbon

The functional group availability on the surface sample was recorded by Fourier-transform infrared spectrophotometer IR-Affinity-1 (SHIMADZU CORP), available at RTMNU, Nagpur. A broad peak at 3,329.43 cm^{-1} corresponds to free phenolic –OH stretching which is attributed to the –OH group of alcohols, carboxyl and phenols. The peaks at 1,000–1,200 cm^{-1} show

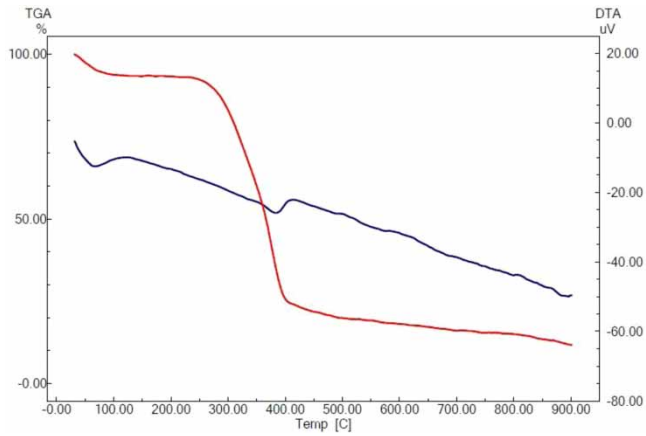

Figure 3 | TGA-DTA curve of raw bagasse.

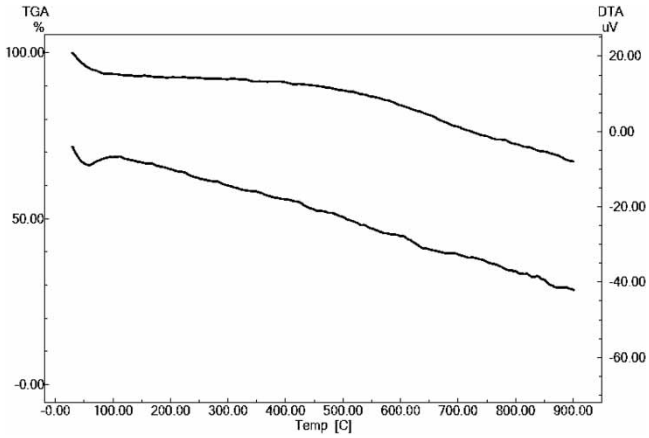

Figure 4 | TGA-DTA curve of char.

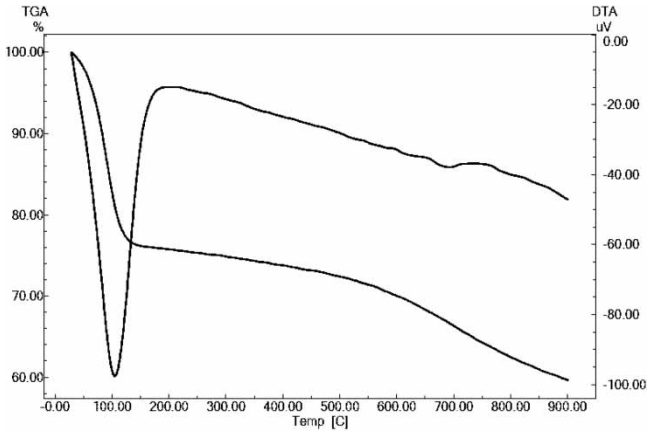

Figure 5 | TGA-DTA curve of activated carbon (SB-Zn_2-900).

the existence of a phenolic and alcoholic group which is identified in raw bagasse. The FTIR spectra of raw SB is shown in Figure 6.

FTIR spectra of char at 1,711.65 and 1,568.96 cm^{-1} corresponds to the –C = O group stretching of carboxylic acid. The band at 1,089.79 cm^{-1} indicates the presence of a primary amine. The FTIR spectra of bagasse char is shown in Figure 7.

FTIR spectra of $ZnCl_2$ activated carbon shows peaks around 3,600–3,700 cm^{-1} which corresponds to free phenolic –OH stretching which is attributed to the –OH group of alcohols, carboxyl and phenols. This band is not observed in char corresponding to structure decomposition and hydroxyl group removal. The bands obtained between 2,857 and 3,000 cm^{-1} are due to symmetric and asymmetric C–H vibrations. The band at 2,926.38 cm^{-1} shows methylene C–H stretching. This peak does not exist in char. The band around 1,747.58 cm^{-1} shows the presence of a C–O double bond group. The band at 1,555.27 cm^{-1} informing aromatic C = C ring. The peaks at 1,000–1,200 cm^{-1} show the existence of phenolic and alcoholic groups which are identified in raw bagasse, char and activated carbon. The peaks around 600–900 cm^{-1} denote the existence of an aromatic ring structure which is observed in raw bagasse, char and activated carbon. The transmittance at 1,000–1,300 cm^{-1} was observed in raw bagasse only which corresponds to C–O stretching in ethers. After activation of bagasse, C = O stretching in aldehydes, ketones and C–O stretch in ethers disappeared in the same fashion as reported by Guo & Lua (2000). At high temperature C–O and C = O groups were removed, forming polyaromatic structures (Li *et al.* 2008; Abdul Hamid *et al.* 2014).

It is proven from the FTIR spectra that raw bagasse and char show much less functional groups. The appearance of functional groups occurred by chemical activation at various temperatures. The activated carbon was found to contain aliphatic, aromatic and oxygen-containing functional groups. The FTIR spectra of activated carbon is shown in Figure 8.

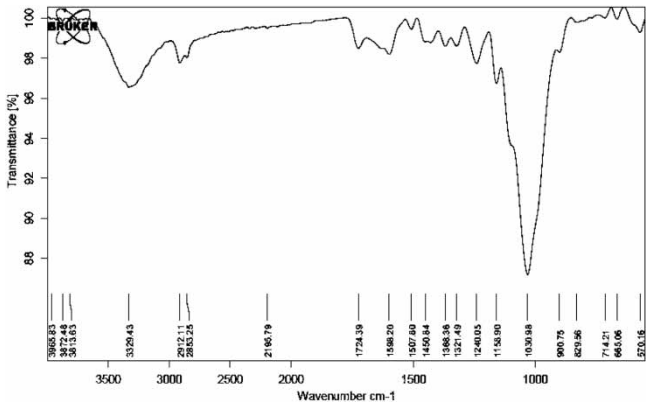

Figure 6 | FTIR spectra of raw bagasse.

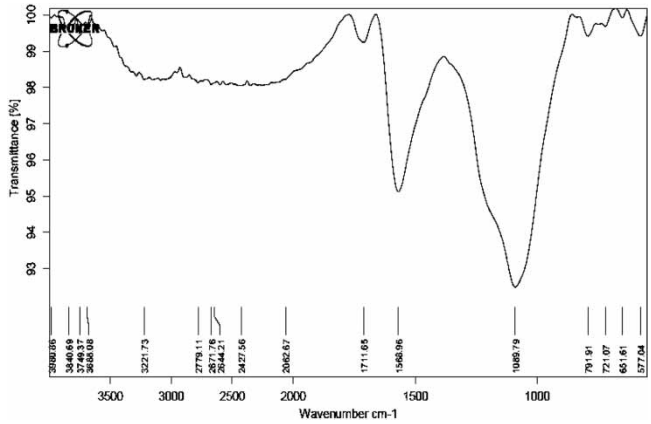

Figure 7 | FTIR spectra of char.

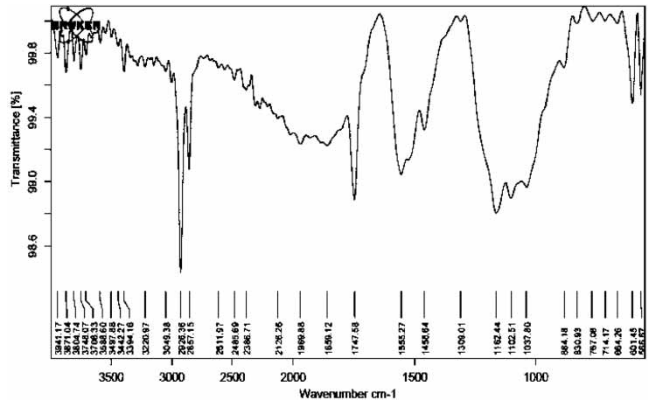

Figure 8 | FTIR spectra of activated carbon (SB-Zn_2-900).

4.2.5. XRD of raw bagasse, char and activated carbon

Structural analysis was carried out by powder XRD studies. XRD study was carried out by using 'Rigaku' (Miniflex) diffractrometer, available at RUSA, Nagpur. XRD studies show the amorphous or crystalline nature of materials. X-ray scattering is an analytical technique which gives information about the crystallographic structure, chemical composition and physical properties of materials. These techniques are based on detecting the scattered intensity of an X-ray beam hitting a sample as a function of incident and scattered angle, polarization and wavelength or energy (Pradhan 2011).

Crystalline material shows sharp peaks while amorphous material shows a single broad diffused peak. The diffraction spectra was recorded at the rate of 0.02 °C. The angle range (2θ) was investigated between 0 and 70 °C. XRD pattern of raw bagasse is shown in Figure 9.

XRD data of bagasse char show the amorphous nature of char with no sharp peaks. The XRD spectra is shown in Figure 10.

The XRD spectra of activated carbon confirms the amorphous nature of activated carbon. The XRD spectra of activated carbon is shown in Figure 11.

4.2.6. SEM of raw bagasse, char and activated carbon

The surface morphology of activated carbon was studied by scanning electron microscope. The SEM gives an indication of the nature of porosity. A SEM is a type of electron microscope that scans a sample with a high-energy electron beam. The electrons interact with the atoms of the sample thereby producing signals which tell about the surface structure of the sample, its composition and other properties such as electrical conductivity. In the SEM technique, the sample was coated with gold for good conductivity. Surface morphology was obtained by magnifying the real image 1,200 times (Pradhan 2011). The scanning electron microscope used was the JEOL-6380A model available at VNIT, Nagpur.

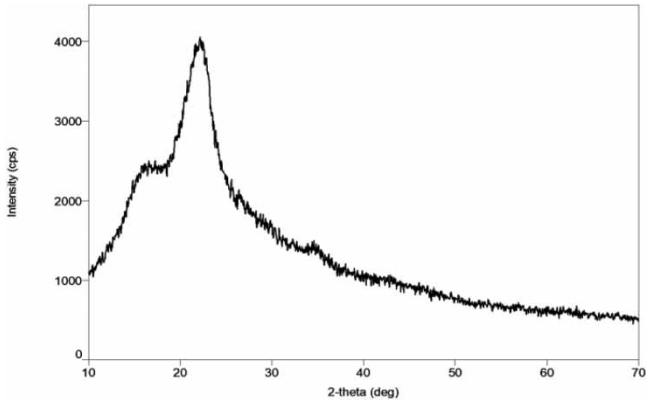

Figure 9 | XRD pattern of raw bagasse.

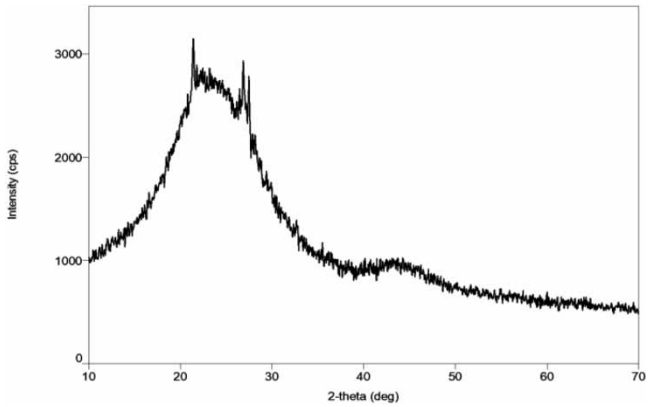

Figure 10 | XRD pattern of char.

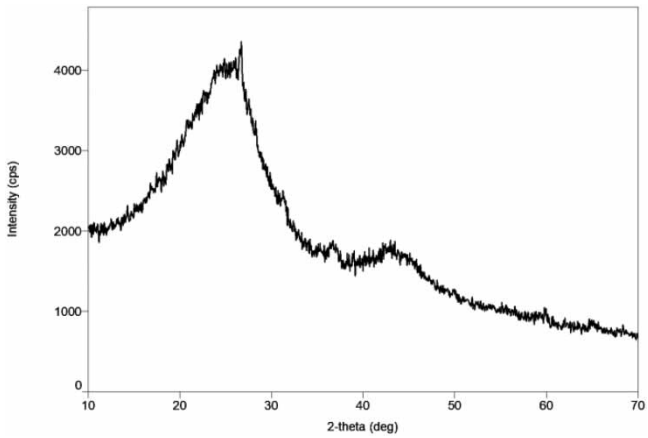

Figure 11 | XRD pattern of activated carbon (SB-Zn_2-900).

It can be observed from the micrographs that no pores were observed on the surface of raw bagasse. The SEM images of raw bagasse is shown in Figure 12.

During char formation, volatiles are removed thereby producing pores on the char surface. The SEM image of bagasse char is shown in Figure 13.

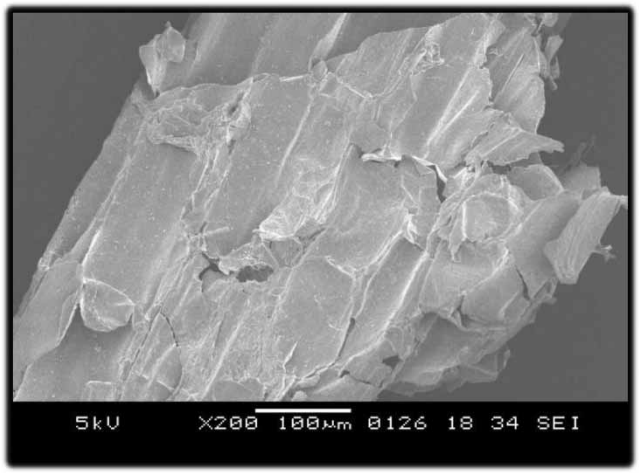

Figure 12 | SEM image of raw bagasse.

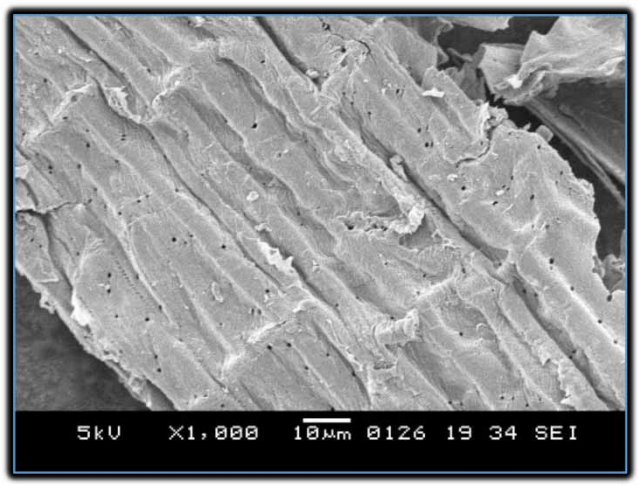

Figure 13 | SEM image of bagasse char.

More cavities and a wider pore network were observed on the activated carbon surface (Hanum *et al.* 2017). It is concluded from SEM images that chemical activation leads to the formation of pores and widening of existing pores. This confirms the porous nature of activated carbon. The SEM image of activated carbon SB-Zn_2-900 is shown in Figure 14.

4.2.7. BET surface area of raw bagasse, char and activated carbon

BET surface area analysis is the multi-point measurement of specific surface area through gas adsorption analysis in which an inert gas nitrogen is continuously flown over a solid sample of activated carbon. Small gas molecules adsorb to the solid substrate and its porous structures due to weak van der Waals forces, forming a monolayer of adsorbed gas. This monomolecular layer and rate of adsorption can be used to calculate the specific surface area of a solid sample (Pradhan 2011). It was determined by QUANTACHROME (Nova-Touch) surface area analyzer available at RTMNU, Nagpur.

The raw bagasse has 0 m^2/g of surface area with a pore volume 0.4771 cc/g. The linear isotherm of adsorption–desorption of nitrogen for raw bagasse is shown in Figure 15.

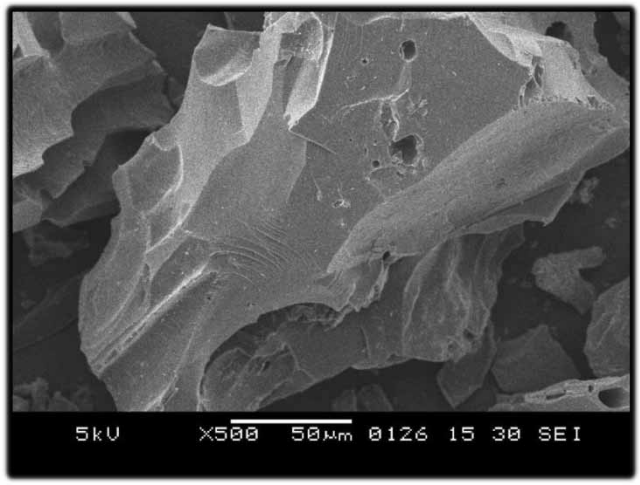

Figure 14 | SEM image of activated carbon (SB-Zn_2-900).

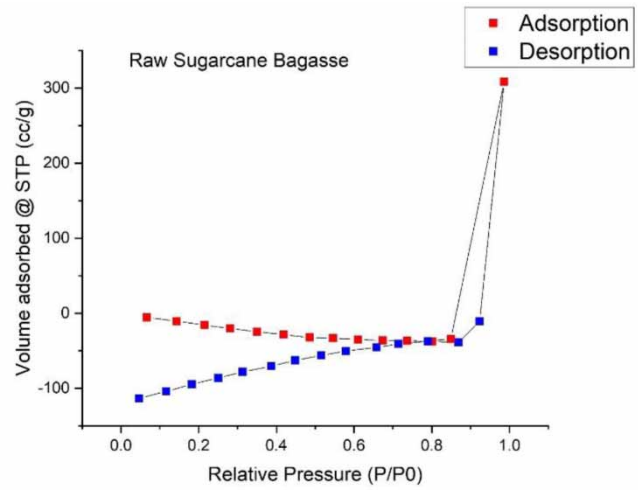

Figure 15 | Linear isotherm of raw bagasse char.

The surface area of bagasse char at 900 °C obtained was 514.27 m^2/g with a total pore volume of 0.4090 cc/g. This confirms that charrification of raw material can improve porousness and thereby surface area. The linear isotherm of adsorption-desorption of nitrogen for bagasse char is shown in Figure 16.

The surface area of zinc chloride-activated SB was found to be 1,386.58 m^2/g with a total pore volume of 0.9947 cc/g. The comparative table of surface areas of raw bagasse, its char and activated carbon is shown in Table 4. The linear isotherm of adsorption–desorption of nitrogen for activated carbon is shown in Figure 17.

4.3. Energy-dispersive spectroscopy analysis of raw bagasse, char and activated carbon

EDS is an analytical technique used for the elemental analysis or chemical characterization of a sample. It was determined with SEM by the JEOL-6380A instrument available at VNIT, Nagpur.

The EDS analysis of raw bagasse, char and activated carbon is shown in Table 5. It was revealed from the EDS studies that raw bagasse contains 56.25% C, 42.22% O, 0.79% Pt, 0.42% Si and 0.33% Al. SB after carbonization contains 81.87% C, 16.72% O, 0.44% Pt, 0.53% Si and 0.45% Ca. Activated carbon produced after chemical activation with zinc chloride contains

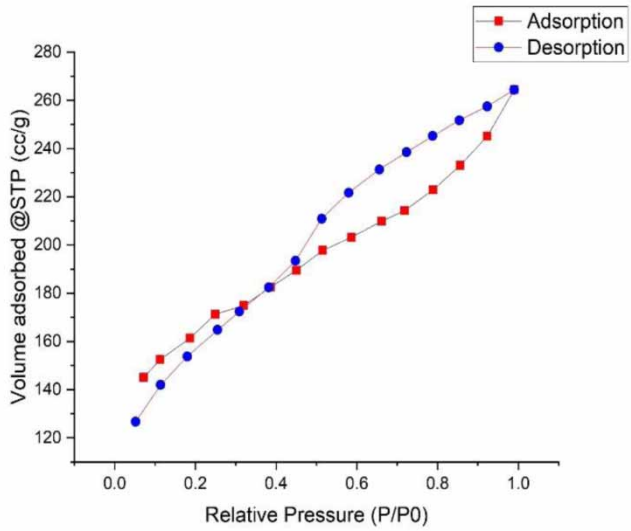

Figure 16 | Linear isotherm of char.

Table 4 | BET surface area, pore volume and size

Sample	BET surface area (m^2/g)	V_{tot} (cm^3/g)	Avg. pore size (A°)
Raw SB	0.00	0.4771	–
SB Char	514.270	0.4090	15.907
SB-Zn_2-900[a]	**1,386.58**	**0.9947**	**15.507**

[a]Bold indicates that activated carbon has the highest surface area, pore volume and pore size compared with raw material and its char.

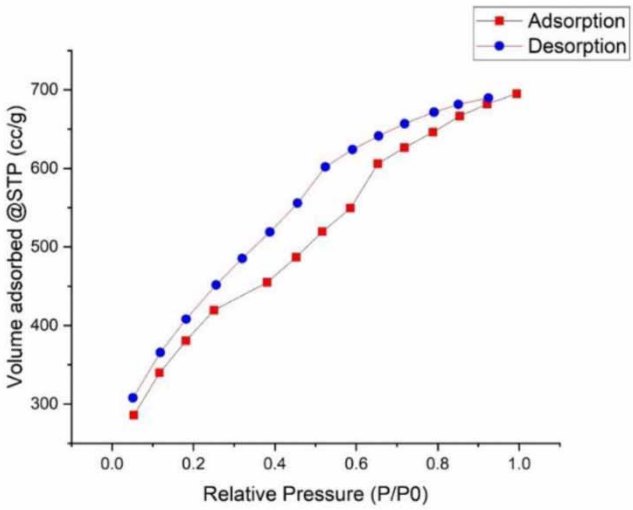

Figure 17 | Linear isotherm of SB-Zn_2-900.

74.50% C, 12.27% O, 0.22% Pt, 0.04% Si, 12.17% N, 0.52% Cl and 0.20% Zn. These results revealed that after carbonization the char and activated carbon met the requirement of 65% C as per SNI No. 06-3730-1995 (Guo & Lua 2000; Adlim *et al.* 2021).

The comparative study of raw material, activating agent used, condition of activation, CHN analysis, iodine number and BET surface area with previous research studies is shown in Table 6.

Table 5 | Elemental analysis

Sample name	% C	% O	% Pt	% Si	% Al	% Ca	% N	% Cl	%Zn
Raw bagasse	56.25	42.22	0.79	0.42	0.33	–	–	–	–
Bagasse char	81.87	16.72	0.44	0.53	–	0.45	–	–	–
SB-Zn_2-900	74.50	12.27	0.22	0.04	–	–	12.17	0.52	0.20

Table 6 | Comparative study with the previous research

Raw material	Activating agent	Optimum impregnation ratio/temperature (°C)	% C	% H	% N	Iodine no. (mg/g)	BET surface area (m^2/g)	Reference
Safflower seed press cake	$ZnCl_2$	4:1/900	76.29	2.26	2.48	128.21	801.5	Lua & Ting (2004)
Sugarcane bagasse	$ZnCl_2$	1:1/400	–	–	–	868	–	Joshi & Vishnu (2020)
Sugarcane bagasse	$ZnCl_2$	5:1/500	–	–	–	–	905	Tsai *et al.* (2001)
Sugarcane bagasse	$ZnCl_2$	2:1/900				277.78	1,302.4	Nemr *et al.* (2021)
Sugarcane bagasse	$ZnCl_2$	2:1/600				239.6	831	Cai *et al.* (2019)
Mangrove waste	H_3PO_4	4:1/300	94.18	2.83	–	72.3	1,011.8	Zakaria *et al.* (2021)
Rice husk	H_3PO_4	500	–	–	–	–	420	Njewa *et al.* (2022)
Marula nutshell	H_3PO_4	500	–	–	–	1,075.7	–	Mkungunugwa *et al.* (2021)
Kenaf core fiber	H_3PO_4	1:4/500	–	–	–	–	299.02	Shamsuddin *et al.* (2016)
Mangrove charcoal	H_3PO_4	725	–	–	–	1,019.87	354.97	Budianto *et al.* (2019)
Olive stone	H_3PO_4	500	–	–	–	–	1,218	Yakout & El-Deen (2012)
Palm kernel shell	KOH	1.5:1/800	61.10	1.40	0.00	994.83	–	Andas *et al.* (2017)
Bamboo stem	KOH	3:1/800	79.11	1.60	0.10	–	726	Khalil *et al.* (2013)
Sugarcane bagasse	$ZnCl_2$	2:1/900	80.126	3.569	1.873	1,140.69	1,386.58	This study

5. CONCLUSIONS

This study investigated the preparation of activated carbon from naturally available bio-waste material SB. In this study, the characterization results of CHN analysis, FTIR, XRD, BET surface area and SEM analysis of raw bagasse, bagasse char and zinc chloride-impregnated activated carbon were compared. From the results, it was observed that more activation temperature gives lesser yield of the product. It means product yield is inversely proportional to the activation temperature. The iodine number gives an indication about the porousness of activated carbon. Higher iodine numbers mean highly porous carbon. The iodine numbers of SB-Zn_2-900 and char at 900 °C were found to be 1,140.69 and 510.75 mg/g, respectively. The CHN analysis data reveal that activation of raw material can transform into activated carbon with carbon % of 42.049, 48.150 and 80.126 for raw bagasse, its char and activated carbon. The FTIR study investigated that raw bagasse and char shows very less functional groups. The appearance of functional groups occurred by chemical activation at various temperatures. The activated carbon was found to contain aliphatic, aromatic and oxygen-containing functional groups. From SEM micrographs, it is concluded that there are very less pores in raw bagasse, some pores were seen in char and a large number of pores

were observed in SB-Zn_2-900. It means activation with the chemical agent can impart porousness in the carbon. The BET surface area of SB-Zn_2-900, char and raw bagasse was found to be 1,386.58, 514.270 and 0 m^2/g, respectively, which shows raw bagasse does not exhibit adsorption properties. On the other hand, char has less and activated carbon has a larger adsorption capacity. The optimum ratio of impregnation and activation temperature was found to be 1:2 at 900°. Elemental analysis was also carried out by EDS and showed that char contains 81.87% C whereas activated carbon contains 74.50% C. However, SB can produce good surface area carbon that can be utilized for further adsorption studies.

AVAILABILITY OF DATA AND MATERIALS

All the data are available in the manuscript

AUTHORS' CONTRIBUTIONS

E.R.R. carried out the collection of biomaterials, synthesis, characterization and preparation of manuscript. M. A. B. and A. R. C. carried out the concept and guidance of research work.

DATA AVAILABILITY STATEMENT

All relevant data are included in the paper or its Supplementary Information.

CONFLICT OF INTEREST

The authors declare there is no conflict.

REFERENCES

Abdul Hamid, S. B., Chowdhury, Z. Z. & Zain, S. M. 2014 Base catalytic approach: a promising technique for the activation of biochar for equilibrium sorption studies of copper Cu(II) ions in single solute system. *Materials* **7**, 2815–2832.

Adlim, M., Ratu, F. I. R., Fitri, Z., Latifah, H., Maily, R., Nurul, U. M. & Omar, M. 2021 Simple preparations and characterizations of activated-carbon- clothes from palm-kernel-shell for ammonia vapor adsorption and skim-latex-odor removal. *Indonesian* Journal of Chemistry **21** (4), 920–931.

Andas, J., Rahman, M. L. A. & Yahya, M. S. M. 2017 Preparation and characterization of activated carbon from palm kernel shell. *IOP Conference Series: Materials Science and Engineering* **226**, 012156. doi:10.1088/1757-899X/226/1/012156.

Angın, D., Altintig, E. & Kose, T. E. 2013 Influence of process parameters on the surface and chemical properties of activated carbon obtained from biochar by chemical activation. *Bioresource Technology* **148**, 542–549. http://dx.doi.org/10.1016/j.biortech.2013.08.164.

Bouchemal, N., Belhachemi, M., Merzougui, Z. & Addoun, F. 2015 The effect of temperature and impregnation ratio on the active carbon porosity. *Desalination and Water Treatment* **10** (1–3), 115–120.

Budianto, A., Kusdarini, E., Effendi, S. S. W. & Aziz, M. 2019 The production of activated carbon from Indonesian mangrove charcoal. *IOP Conference Series: Materials Science and Engineering* **462** (1–8), 012006. doi:10.1088/1757-899X/462/1/012006.

Cai, Y., Liu, L., Tian, H., Yang, Z. & Luo, X. 2019 Adsorption and desorption performance and mechanism of tetracycline hydrochloride by activated carbon-based adsorbents derived from sugar cane bagasse activated with $ZnCl_2$. *Molecules* **24** (24), 4534–4551. https://doi.org/10.3390/molecules24244534.

Cartula, F., Molina-Sabio, M. & Rodriguez-Reinoso, F. 1990 Preparation of activated carbon by chemical activation with $ZnCl_2$. *Carbon* **29** (7), 99–1107.

Chisutia, W. W., Mmari, O. J. & Mwanza, S. P. 2014 Adsorption of Congo Red Dye from aqueous solutions using roots of *Eichhornia crassipes*: kinetic and equilibrium studies. *Energy Procedia* **50**, 862–869.

Dantas, G. A., Legey, L. F. & Mazzone, A. 2013 Energy from sugarcane bagasse in Brazil: an assessment of the productivity and cost of different technological routes. *Renewable and Sustainable Energy Reviews* **21**, 356–364.

Demiral, H., Demiral, I., Tümsek, F. & Karabacakoglu, B. 2008 Pore structure of activated carbon prepared from hazelnut bagasse by chemical activation. *Surface and Interface Analysis* **40**, 616–619.

Dwiyaniti, M., Barruna, E. A. G., Naufal, M. R., Subiyanto, I., Setiabudy, R. & Hudaya, C. 2020 Extremely high surface area of activated carbon originated from sugarcane bagasse. *Materials Science and Engineering* **909**, 012018.

Ekpete, O. A., Marcus, A. C. & Osi, V. 2017 Preparation and characterization of activated carbon obtained from Plantain (*Musa paradisiaca*) fruit stem. *Journal of Chemistry* **2017**, 8635615. https://doi.org/10.1155/2017/8635615.

Foo, K. Y. & Hameed, B. H. 2011 Preparation and characterization of activated carbon from pistachio nut shells via microwave-induced chemical activation. *Biomass and Bioenergy* **35**, 3257–3261.

Gardare, V. N., Yadav, S., Avhad, D. N. & Rathod, V. K. 2015 Preparation of adsorbent using sugarcane bagasse by chemical treatment for the adsorption of methylene blue. *Desalination and Water Treatment* **56**, 2872–2878.

Ghani, Z. A., Yusoff, M. S., Zaman, N. Q., Zamri, M. F. M. A. & Andas, J. 2017 Optimization of preparation conditions for activated carbon from banana pseudo-stem using response surface methodology on removal of color and COD from landfill leachate. *Waste Management* **62**, 177–187.

Guo, J. & Lua, A. C. 2000 Preparation and characterization of adsorbents from oil palm fruit solid wastes. *Journal of Oil Palm Research* **12**, 64–70.

Hamza, U. D., Nasri, N. S., Amin, N. S., Mohammed, J. & Zain, H. M. 2015 Characteristics of oil palm shell biochar and activated carbon prepared at different carbonization times. *Desalination and Water Treatment* **57** (17), 1–8.

Hanum, F., Bani, O. & Wirani, L. I. 2017 Characterization of activated carbon from rice husk by HCl activation and its application for lead (Pb) removal in car battery wastewater. *IOP Conference Series: Materials Science and Engineering* **180**, 012151.

Harry, M. & Francisco, R. R. 2006 Production and reference material. In: Marsh, H. & Reinoso, F. R. (eds), *Activated Carbon*. Elsevier Science Ltd, Amsterdam, The Netherlands.

Hayashi, J., Horikawa, T., Muroyama, K. & Gomes, V. G. 2002 Activated carbon from chickpea husk by chemical activation with K_2CO_5: preparation and characterization. *Microporous and Mesoporous Materials* **55**, 63–68.

Hock, P. E. & Zaini, M. A. A. 2018 Activated carbons by zinc chloride activation for dye removal – a commentary. *Acta Chimica Slovaca* **11** (2), 99–106. doi: 10.2478/acs-2018-0015.

Hofsetz, K. & Silva, M. A. 2012 Brazilian sugarcane bagasse: energy and non-energy consumption. *Biomass and Bioenergy* **46**, 564–573.

Hon, D. N. S. & Shiraishi, N. M. D. 2000 *Wood and Cellulosic Chemistry*, 2nd edn. CRC Press, Boca Raton, FL, USA.

Ioannidou, O. & Zabaniotou, A. 2007 Agricultural residues as precursors for activated carbon production – a review. *Renewable and Sustainable Energy Reviews* **11**, 1966.

Joshi, S. & Vishnu, K. C. 2020 Synthesis and characterization of sugarcane bagasse based activated carbon: effect of impregnation ratio of $zncl_2$. *Journal of Nepal Chemical Society* **41** (1), 74–79.

Kalderis, D., Bethanis, S., Paraskeva, P. & Diamadopoulos, E. 2008 Production of activated carbon from bagasse and rice husk by a single-stage chemical activation method at low retention times. *Bioresource Technology* **99**, 6809–6811.

Khalil, H. P. S. A., Jawaid, M., Firoozian, P., Rashid, U., Islam, A. & Akil, H. M. 2013 Activated carbon from various agricultural wastes by chemical activation with KOH: preparation and characterization. *Journal of Biobased Materials and Bioenergy* **7**, 1–7.

Kumar, A. & Bhattacharya, T. 2018 Biochar and its application. In *Conference: Biogeochemical Cycles and Climate Change*, pp. 1–17.

Li, W., Yang, K., Peng, J., Zhang, L., Guo, S. & Xia, H. 2008 Effects of carbonization temperatures on characteristics of porosity in coconut shell chars and activated carbons derived from carbonized coconut shell chars. *Industrial Crops and Production* **28**, 190–198.

Lua, A. C. & Ting, Y. 2004 Effect of activation temperature on the textural and chemical properties of potassium hydroxide activated carbon prepared from pistachio-nut shell. *Journal of Colloid and Interface Science* **274**, 594–601.

Michael, B., Claudia, K. & William, M. 2017 *Analysis of Biochars for C, H, N, O and S by Elemental Analyser*. Available from: https://www.researchgate.net/publication/315838304.

Misran, E., Maulina, S., Dina, S. F., Nazar, A. & Harahap, S. A. 2018 Activated carbon production from bagasse and banana stem at various times of carbonization. *Materials Science and Engineering* **309**, 012064.

Mkungunugwa, T., Manhokwe, S., Chawafambira, A. & Munyaradzi, S. 2021 Synthesis and characterisation of activated carbon obtained from Marula (*Sclerocarya birrea*) nutshell. *Journal of Chemistry* **2021**, 5552224. https://doi.org/10.1155/2021/5552224.

Naik, S. N., Goud, V. V., Rout, P. K. & Dalai, A. K. 2010 Production of first and second generation biofuels: a comprehensive review. *Renewable and Sustainable Energy Reviews* **14**, 578–597.

Nemr, A. E., Aboughaly, R. M., Sikaily, A. E., Ragab, S., Masoud, M. S. & Ramadan, M. S. 2021 Utilization of sugarcane bagasse/$ZnCl_2$ for sustainable production of microporous nano-activated carbons of type I for toxic Cr(VI) removal from aqueous environment. *Biomass Conversion and Biorefinery* **13** (5), 1–20. https://doi.org/10.1007/s13399-021-01445-6.

Njewa, J. B., Vunain, E. & Biswick, T. 2022 Synthesis and characterization of activated carbons prepared from agro-wastes by chemical activation. *Journal of Chemistry* **1–13**, 9975444. https://doi.org/10.1155/2022/9975444.

Nunes, L. J. R., Loureiro, L. M. E. F., Sá, L. C. R. & Silva, H. F. C. 2020 Sugarcane industry waste recovery: a case study using thermochemical conversion technologies to increase sustainability. *Applied Science* **10** (18), 1–17.

Obi, F. O., Ugwuishiwu, B. O. & Nwakaire, J. N. 2016 Agricultural waste concept, generation, utilization and management. *Nigerian Journal of Technology (NIJOTECH)* **35** (4), 957–964.

Oubagaranadin, J. U. K. & Murthy, Z. V. P. 2012 *Activated Carbons: Classifications, Properties and Applications, Chapter 6*. Nova Science Publishers, Inc., New York.

Paraskeva, P., Kalderis, D. & Diamadopoulos, E. 2008 Review – production of activated carbon from agricultural by-products. *Journal of Chemical Technology and Biotechnology* **83**, 581–591.

Pradhan, S. 2011 *Production and Characterization of Activated Carbon Produced From A Suitable Industrial Sludge. A Project Report*. NIT Rourkela.

Ramajo-Escalera, B., Espina, A., García, J., Sosa-Arnao, J. & Nebra, S. 2006 Model-free kinetics applied to sugarcane bagasse combustion. *Thermochimica Acta* **448**, 111–116.

Rashed, M. N., 2013 Adsorption technique for the removal of organic pollutants from water and wastewater book, Chapter 7. In: *Organic Pollutants – Monitoring, Risk and Treatment* (Rashed, M. N., ed.). IntechOpen. Available from: https://www.intechopen.com

Raut, E., Bedmohata, M. & Chaudhari, A. R. 2021 A review on toxic metal ions removal by using activated carbon prepared from natural biomaterials. *Journal of Physics* **1913**, 012091.

Rezende, C. A., Lima, M. A., Maziero, P., DeAzevedo, E. R., Garcia, W. & Polikarpov, I. 2011 Chemical and morphological characterization of sugarcane bagasse submitted to a delignification process for enhanced enzymatic digestibility. *Biotechnology and Biofuels* **4** (54), 1.

Salgado, M. D. F., Abioye, A. M., Junoh, M. M., Santos, J. A. P. & Ani, F. N. 2018 Preparation of activated carbon from babassu endocarpunder microwave radiation by physical activation. *Earth and Environmental Science* **105**, 012116. doi:10.1088/1755-1315/105/1/012116.

Samariha, A. & Khakifirooz, A. 2011 Application of NSSC pulping to sugarcane bagasse. *BioResources* **6**, 3313–3323.

Shamsuddin, M. S., Yusoff, N. R. N. & Sulaiman, M. A. 2016 Synthesis and characterization of activated carbon produced from kenaf core fiber using H_3PO_4 activation. *Procedia Chemistry* **19**, 558–565. doi:10.1016/j.proche.2016.03.053.

Standard Test Method 2006 *Standard Test Method for Determination of Iodine Number of Activated Carbon, Designation: D 4607-94 (Reapproved 2006)*. ASTM International, West Conshohocken, PA, USA.

Tsai, W. T., Chang, C. Y., Lin, M. C., Chien, S. F., Sun, H. F. & Hsieh, M. F. 2001 Characterization of activated carbons prepared from sugarcane bagasse by ZnCl2. *Journal of Environmental Science and Health, Part B* **36** (3), 365–378. doi:10.1081/PFC-100103576.

Wereko-Brobby, C. Y. & Hagen, E. B. 1996 *Biomass Conversion and Technology*. John Wiley and Sons, New York.

Yakout, S. M. & El-Deen, G. S. 2012 Characterization of activated carbon prepared by phosphoric acid activation of olive stones. *Arabian Journal of Chemistry* **9** (2), S1155–S1162. https://doi.org/10.1016/j.arabjc.2011.12.002.

Zakaria, R., Jamalluddin, N. A. & Bakar, M. Z. A. 2021 Effect of impregnation ratio and activation temperature on the yield and adsorption performance of mangrove based activated carbon for methylene blue removal. *Results in Materials* **10**, 100183. https://doi.org/10.1016/j.rinma.2021.100183.

First received 23 December 2022; accepted in revised form 29 March 2023. Available online 2 May 2023